Fabrication and characterization of nanomechanical properties of double-quantum-dot-based qubits in carbon nanotubes

Author: Núria Urgell Ollé and
Advisor: Adrian Bachtold
*ICFO-Institut de Ciències Fotòniques, Mediterranean Technology Park, Avinguda Carl Friedrich Gauss, 3, 08860 Castelldefels, Barcelona**

Advisor: Antoni García-Santiago
Facultat de Física, Universitat de Barcelona, Diagonal 645, 08028 Barcelona, Spain.

Abstract: Carbon nanotubes possess quantum properties that make them promising candidates to be used to control and achieve charge qubits. In this paper, we present a remarkable fabrication method to achieve clean low-resistance carbon nanotubes with integrated double quantum dots and a quantum sensor dot. The nanomechanical properties of such a system are studied and a measurement method for detecting single suspended carbon nanotubes in the devices is discussed and efficiently integrated.

I. INTRODUCTION

Carbon atoms can arrange in different crystalline structures. There are numerous allotropes of carbon, such as diamond, graphene, or carbon nanotubes (CNTs). Since their recent discovery in 1991 by Iijima [1], CNTs have been studied for their unique electrical and mechanical properties. Based on these properties, CNTs are being used as supercapacitors, field-effect transistors, or quantum bits, the so-called qubits [2]. In this paper we focus on the study of double quantum dots defined in CNTs that can be used as mechanical qubits. This work was completed at the Institute of Photonic Sciences (ICFO) in the Quantum NanoMechanics group, which focuses on the study of the quantum-mechanical properties of nanomaterials such as CNTs and twisted bilayer graphene.

CNTs can be classified according to their atomic structure and electrical properties. CNTs can be understood as rolled-up graphene sheets. Since there are infinite ways of rolling up a sheet, there are infinite nanotube structures that vary in diameter and atomic geometry. Thus, we can classify CNTs as armchair, zigzag and chiral according to the symmetries of their atomic structure. Additionally, based on their electronic properties CNTs can be classified as metallic or semiconducting [2].

There are various synthesis methods for CNTs: laser ablation, chemical vapor deposition (CVD), and arc-discharge. Laser ablation and arc-discharge methods require subsequent processing of the devices after growth which is a disadvantage in comparison with the CVD method. The latter allows better control of CNT characteristics such as average diameter and length and allows for growth in multiple substrates. The CVD method requires tuning various parameters such as temperature, gas flow through the tube, amount and type of catalysts, which affect the quantity and quality of the produced CNTs [3].

CNTs are structures that offer electrical, mechanical, and quantum properties that make them suited to be used as qubits. A qubit is a two-state quantum system and the basic unit of information in quantum computing. An approach to obtaining a two-state quantum system in CNTs is the formation of double quantum dots (DQD). Quantum dots (QDs) are semiconductor nanostructures that confine particles in space. A particle confined in a potential has a discrete energy spectrum and thus QDs have quantized energy spectra. In CNTs electrons are confined to one dimension, thus when a semiconducting CNT is suspended between two electrical contacts electrons are confined to a point in space and QDs are formed. Additionally, a gate is capacitively coupled to the CNT and enables the tuning of the electrostatic potential. A DQD is formed connecting two QDs in series within one CNT. Thus, for full control of the DQD system, five gates capacitively coupled to the CNT are needed (see Fig. 1a) [4][5].

Fabrication of gated CNT quantum devices takes different approaches: top gating, bottom gating, and mechanical transfer. Top gating involves fabricating the gates on top of the CNT, whereas bottom gating requires the growth of CNTs on prefabricated electrodes. A drawback of top gating is that the process can damage the cleanliness of the CNT, which is crucial for sensitive measurements. The mechanical transfer method requires growing the CNTs on a separate chip and transferring a single CNT to the device chip. This process is time-consuming and could also affect the cleanliness of the CNT [2].

For nanomechanical-based qubits, the CNT acts as the resonator body and couples to a force that induces anharmonicity. This force is exerted by electron tunneling on the QD and leads to a discrete energy spectrum. Previously, the Quantum NanoMechanics group has shown that such system couples to the second flexural mode of the CNT, and has proved that the energy difference be-

*Electronic address: urgellnuria@gmail.com

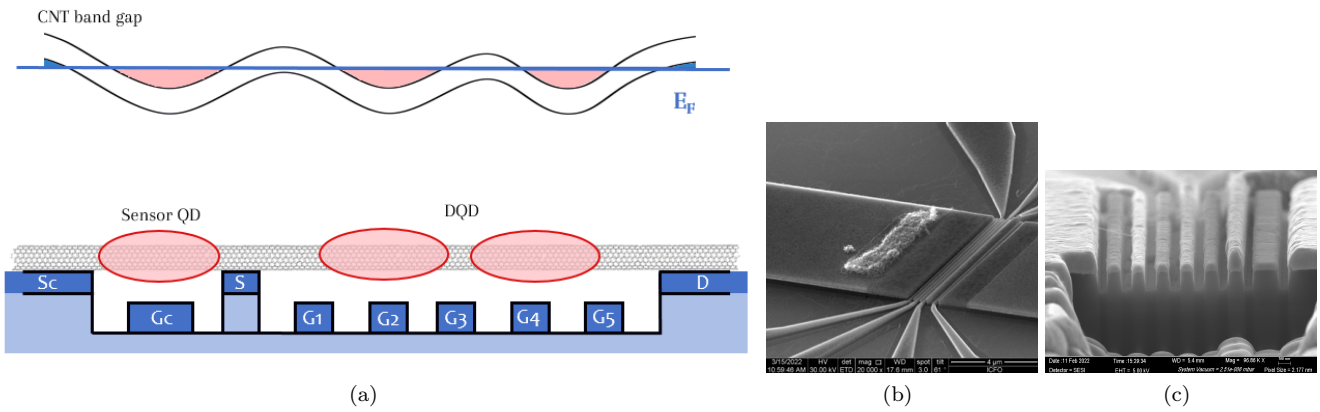

(a) (b) (c)

Figure 1: (a) Device structure. Gate 1 (G1) controls the barrier between the middle source (S) and the first QD, G2, G3, and G4 control the tunnel coupling in the DQD, and G5 controls the barrier between the second QD and the drain (D) (adapted from [7]). Dimensions are not to scale. (b) Scanning Electron Microscope (SEM) images of one device after CVD growth. Catalyst island is on the left. (c) Focused Ion Beam (FIB) image of a device after CVD growth. Sensor QD is on the right.

tween the ground state and first excited states can be effectively used as a qubit [6][7].

This paper focuses on the study of nanomechanical properties of a DQD and sensor QD in a single CNT device and the employed fabrication techniques. The layout of the devices with the addition of the sensor dot was recently incorporated at the Quantum NanoMechanics group. Thus, the aim of this work is to show how to fabricate such devices and ultimately study if the addition of a sensor dot displays an improvement with respect to the current state-of-the-art systems. This work is the first step in the fabrication development of a QD quantum simulator [8].

II. MATERIALS AND METHODS

A. DEVICE STRUCTURE

The starting point of our fabrication is a wafer with prefabricated structures that act as gates, bond pads, and electrodes. The materials used are limited by the high temperatures that the chips need to withstand during the CVD process ($\leq 1050°C$). The chip is a SiO_2 wafer with Ti/Pt electrodes, spin-coated with poly(methyl methacrylate) (PMMA). To allow for the catalyst deposition (shown in subsection II.B) catalyst holes are patterned after the PMMA coating. One chip contains an array of 36 devices as that shown in Fig. 1a. CNTs are grown on the chips by CVD and are suspended between the source (Sc), drain (D), and middle source (S). Five gates (G_i for i$\in \{1, ..., 5\}$) control the DQD and a separate gate (G_c) controls a QD that behaves as a sensor on the same nanotube. The sensor dot is capacitively connected to the closest QD which allows for charge sensing. Such devices contain six separate gates and are referred to as 6-gate devices.

B. FABRICATION PROCESS

1. *CATALYST DEPOSITION*

The catalyst used is an iron(III) nitrate nonahydrate ($Fe(NO_3)_3$), molybdenum (Mo) and aluminum oxide (Al_2O_3) mixture suspended in methanol (CH_3OH). Al_2O_3 particles are big and porous which prevents the aggregation of Fe and Mo, and Mo enhances the catalytic behavior of $Fe(NO_3)_3$.

First, a cleaning step of 40 s in O_2 plasma is needed to remove organic micropollutants. Then, a 15 μl catalyst droplet is placed on the chip and the solvent is dried off on a hotplate at 50°C. Afterward, the excess catalyst is removed by the lift-off procedure. The PMMA layer, which is dissolved in acetone, allows for the removal of the surplus catalyst. For this process, the chips are left in acetone at 50°C for 1 h and pumped afterward. The chips are then transferred to cold acetone and later transferred to 2-propanol to remove the acetone residues. Lastly, the chips are dried-off and the catalyst remains only at the predefined islands on the chip. Table I summarizes the most relevant parameters used.

2. *CHEMICAL VAPOR DEPOSITION*

The CVD process requires the flow of hydrogen (H_2), argon (Ar), and methane (CH_4) gas. First, the chip is cleaned in O_2 plasma for 2 min to ensure it has no contaminants. Then the chips are placed in the tube and the heating process is started. The tube is flushed with argon and hydrogen and the temperature is raised to 1050°C.

Then the growth process is started. The methane valve is opened and the chips are inserted into the oven. In this process the CNT growth takes place and the temperature is dropped to 900°C. The growth process lasts 6 min and stops when the methane valve is closed. The last step is the cool-off process which cools down to room temperature. The parameters used are currently being optimized by the Quantum NanoMechanics group to achieve directional growth of long CNTs (lengths $\geq$ 1,8 μm). CNTs are grown on chips formed by different shaped catalyst islands and then the growth parameters and set-up are changed to statistically study the resulting directions and lengths of CNTs.

Chip instertion temperature	1050°C
Temperature at the start of the growth	900°C
Time of growth	6 min
H_2 rate during growth	100 sccm
Ar rate during growth	500 sccm
CH_4 rate during growth	550 sccm

Table I: Chemical vapor deposition parameters for fast heating technique. The unit sccm stands for "standard cubic centimeter per minute".

C. EXPERIMENTAL SET-UP

The growth yield is analyzed in the in-air probe station and can be found in subsection III.A. Then the devices that present no electrical contact between the source (Sc) and drain (D), nor between the middle source (S) and D (see Fig. 1a) are discarded. The devices that present electrical contact between the sensor dot gate (G_c) or any of the DQD gates (G_i for i$\in \{1, ..., 5\}$) and the drain are also discarded. This step is crucial because the CNTs we are interested in need to be suspended, i.e. the CNTs need to be in electrical contact only with Sc, S, and D (as shown in Fig. 1a) and show mechanical modes at the DQD side. The devices with the required properties are then placed in the vacuum probe station (at a pressure below $3 \cdot 10^{-6}$ bar) and measured. This station allows for probing in a low-noise environment, which is critical for the measurement of the mechanical properties of nanoscale objects.

1. *RESISTANCE TO GATE VOLTAGE MEASUREMENT*

The sketch of the set-up is shown in Fig. 2. One gate is connected to a voltage source that sweeps the voltage from -1.5 V to 1.5 V. Meanwhile the drain is grounded and the source is connected to a lock-in amplifier that sends a 0.02 V signal through a resistor used to determine the resistance of the CNT. The signal is then analyzed by a Python program and the results are plotted. The program plots the resistance of the CNT (R_{CNT}) as a function of the gate voltage and uses the following equations:

$$I = \frac{V_{\text{AB}}}{R} \tag{1}$$

$$I = \frac{V_{\text{in}}}{R + R_{\text{CNT}}} \tag{2}$$

where $V_{\text{in}} = 0.02$ V stands for the suplied voltage by the lock-in amplifier, V_{AB} is the measured voltage between A and B, and $R = 100$ kΩ is the connected resistance (see Fig. 2).

$$\frac{V_{\text{AB}}}{R} = \frac{V_{\text{in}}}{R + R_{\text{CNT}}} \Rightarrow R_{\text{CNT}} = \frac{R \cdot (V_{\text{in}} - V_{\text{AB}})}{V_{\text{AB}}} \tag{3}$$

All components are grounded between measurements to prevent any charge noise from damaging the device. Then all gates are measured and the devices that generate a noise-filled signal are discarded.

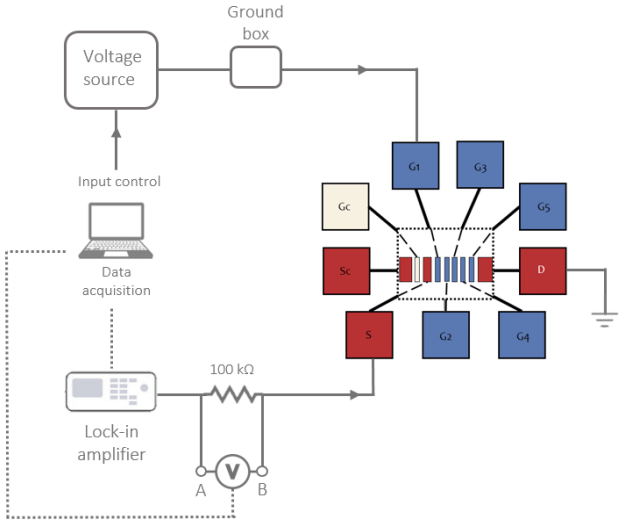

Figure 2: Resistance to gate voltage measurement set-up for gate G_1. The set-up is adapted to modulate the resistance with G_c by connecting S to Sc and D to S.

2. *MECHANICAL MODE MEASUREMENT*

The mechanical mode measurement is only carried out through one gate under the DQD. The gate with the least noisy resistance to gate voltage measurement is selected and using the electrostatic interaction between the gate and the CNT we can detect the motion of the CNT. Sign waves 10 kHz apart are sent using RF signal generators (see Fig. 3). Both generators simultaneously sweep the frequency typically from 10 MHz to 100 MHz at a

given voltage. The addition of an attenuator is crucial for the safety of the CNT. If the output current is well above 50 pA the CNT could vibrate strongly and break. First, an attenuation of -40 dB is applied and the signal is evaluated. If the output current is of the order of the measurement noise ($\approx$ 10 pA) the attenuation is then decreased. Additionally, a bias tee supplies DC current to the RF circuit. Next, after the frequency is swept once, the voltage is increased, and the frequency is swept again. This process is repeated until the voltage reaches the desired value between -1.5 V to 1.5 V. Then a mixer is used to reduce the noise. The software compares the mixed signal with the CNT-mixed signal and discards the non-sine-like noise. Lastly, the drain connects to the lock-in amplifier that reads out the signal. At this step, the devices not showing a mechanical mode are dismissed and studied at the SEM. This process is implemented on rejected devices because the focused beam of electrons produced by the SEM damages the electronic properties of CNTs. Through SEM imaging we can detect the number of CNTs on the device, their shape, and whether they collapsed, which is important for further understanding the devices.

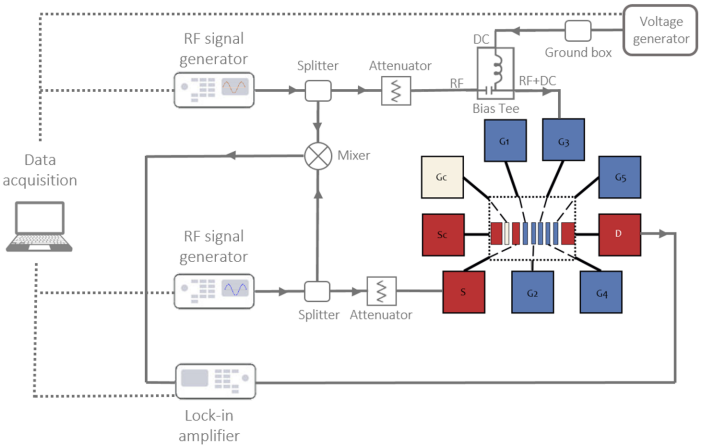

Figure 3: Mechanical mode measurement set-up for gate G_3.

III. RESULTS AND DISCUSSION

A. FABRICATION RESULTS

The in-air probing of the growth yield is compared to the growth yield of single-gate devices, that is devices composed of a single source, gate, and drain. Single-gate devices have been widely studied and successfully implemented by the Quantum NanoMechanics group [9]. Both 6-gate devices and single-gate devices have an equal separation between the source and drain and are fabricated the same way. Thus, both yields should be comparable. The results are plotted in Fig. 4. A total of 432 devices were studied. The average number of devices per chip with and without leaks to the gates with $R_{Sc/D} \in [25k\Omega, 600k\Omega]$ are plotted for all these devices. The average percentage of devices without leaks in the studied resistance range is 4,5% for single-gate devices and 3,1% for 6-gate devices. Considering the low resistance and the cleanliness of our devices, and comparing our yield with established methods we can conclude that our fabrication process has been successfully implemented. To increase the growth yield the Quantum NanoMechanics group is studying the optimization of the growth of CNTs (see subsection II.B.2).

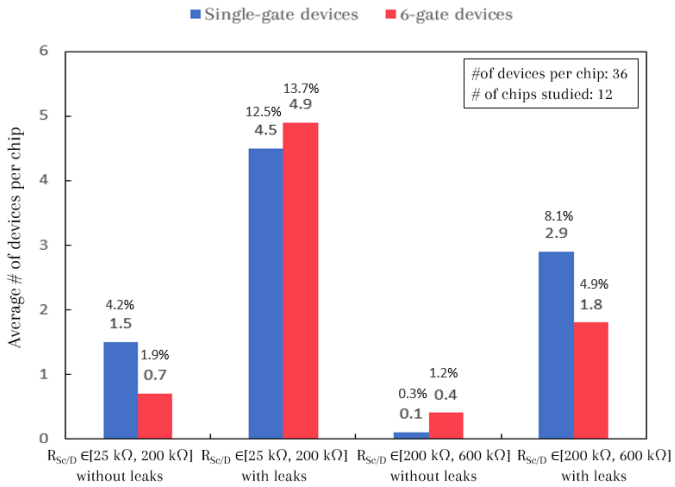

Figure 4: Success statistics of 6-gate devices compared to single-gate devices. Probing of all CNT devices was excuted at the in-air probe station.

B. RESISTANCE TO GATE VOLTAGE

The resistance to gate voltage is plotted in Fig. 5 for gate G_4. The CNT presents a strong modulation of resistance with gate voltage and low resistance (below 150 kΩ). The turning point at 0 V is an intrinsic property of the CNT which indicates that it is semiconducting. The low noise in the signal indicates that we presumably will be able to measure the mechanical mode. Similar results were obtained for the other gates measured.

C. MECHANICAL MODE

The supplied frequency to gate voltage is plotted in Fig. 6. The electrostatic force between the gate and the CNT which induces vibration of the CNT is dependent on the supplied DC gate voltage and a small AC component of the gate voltage. When the supplied frequency matches the CNT resonance frequency we observe a peak in amplitude. Now as the DC voltage on the gate is changed the electrostatic force produces a tension on the

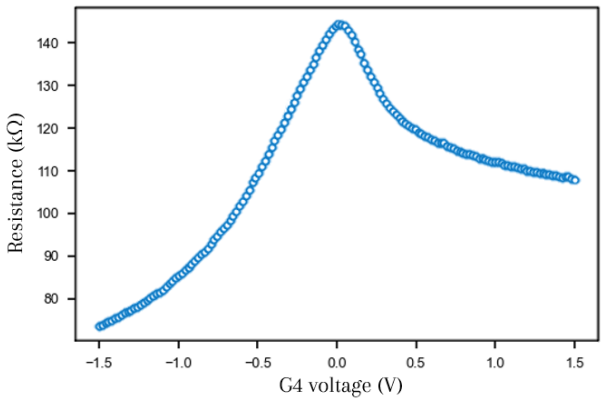

Figure 5: Resistance modulation as a function of gate voltage for gate G_4 (device: C6, chip: G5).

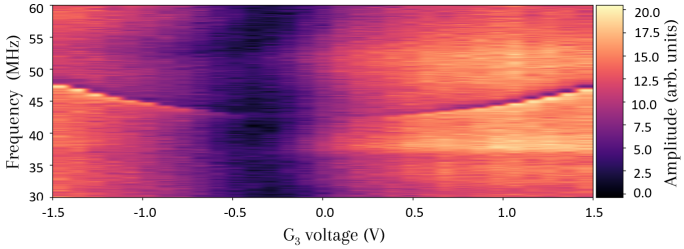

Figure 6: Resonance frequency change given a change in gate (G_3) voltage for device B4 in chip D3. The color gradient indicates the change in amplitude. The curved line at a frequency of ≈ 47 MHz is the mechanical mode.

CNT which tunes the CNTs oscillation frequency [10]. Thus, the mechanical mode can be distinguished as a peak in amplitude that changes frequency with a change in gate voltage. The observation of the mechanical mode allows us to infer that there is a single suspended CNT in the device, crucial for further study of the devices. Therefore as we can observe an amplitude peak in Fig. 6 we can conclude that we have a single vibrating semiconducting CNT clamped to the middle source and drain. Similar results were obtained for the other measured devices.

IV. CONCLUSIONS

This work characterizes the nanomechanical properties of 6-gate devices and allows for the detection of suspended semiconducting CNTs. The resistance to gate voltage measurements are useful for predicting that the CNT is suspended. The following step is to measure devices that show mechanical modes in the dilution fridge at 15 mK and further study the properties of the device. The objective is to obtain the charge stability diagram of the DQD and use the device as a quantum simulator once the theory is developed. At low temperatures, the sensitivity increases, and the charge sensor is expected to be able to detect the mechanical motion of the CNT down to the level of its zero-point motion. Such measurements will determine if the addition of a sensor dot displays an improvement in sensitivity with respect to 5-gate devices. The target is to employ CNT-based sensing dots to carry out real-time measurements of a CNT electromechanical system in the Coulomb-blockade regime at a timescale faster than the mechanical period.

The fabrication has been implemented in a reproducible manner. The suspended CNT devices are low resistance which is crucial for implementing current annealing in the future. We can conclude that our nanofabrication techniques result in high-quality devices.

Acknowledgments

I would like to thank my supervisors Antoni García-Santiago and Adrian Bachtold for their guidance and encouragement. Besides, I would like to acknowledge the SPIE@ICFO Maria Yzuel fellowship awards for the support given during these six months to fulfill the project. Finally, I would like to thank the members of the Quantum Nanomechanics group for their assistance at every stage of the project. Especially, I would like to express my gratitude to Marta Cagetti for her dedicated support throughout the process and for training me at every step.

[1] S. Iijima, *Helical microtubules of graphitic carbon*, Nature 354, 56–58 (1991).
[2] E. Laird et al., *Quantum transport in carbon nanotubes*, Rev. Mod. Phys. 87, 703 (2015).
[3] A. Szabó et al., *Synthesis Methods of Carbon Nanotubes and Related Materials*, Materials 3(5), 3092-3140 (2010).
[4] A. Baydin et al., *Carbon Nanotube Devices for Quantum Technology*, Materials 15(4), 1535 (2022).
[5] S. Sapzman, *Carbon nanotube quantum dots*, PhD Thesis, Technische Universiteit Delft, Delft, Netherlands (2006).
[6] F. Pistolesi et al., *Proposal for a Nanomechanical Qubit*, Phys. Rev. X 11, 031027 (2021).
[7] R. Tormo et al., *Towards a mechanical qubit in a double quantum dot in a carbon nanotube-based device*, QUANTUMatter2022 abstract (2022).
[8] U. Bhattarcharya et al., *Phonon-induced pairing in quantum dot quantum simulator*, Nano Letters 21(22), 9661-9667 (2021).
[9] C. Urgell et al., *Cooling and self-oscillation in a nanotube electromechanical resonator*, Nature Physics 16, 32–37 (2020).
[10] V. Sazonova et al., *A tunable carbon nanotube electromechanical oscillator*, Nature 431, 284–287 (2004).